



α -Fe₂O₃/Reduced Graphene Oxide Nanocomposite: Interfacial Effect on the Magnetic Property

Smhrutisikha Biswal¹ · D. Surya Bhaskaram¹ · G. Govindaraj¹

Received: 20 January 2019 / Accepted: 3 July 2019 / Published online: 17 July 2019
© Springer Science+Business Media, LLC, part of Springer Nature 2019

Abstract

In the present work, the α -Fe₂O₃/RGO nanocomposite is synthesized by one-pot solvothermal technique. The structural analysis is accomplished using X-ray diffraction and Raman spectroscopy. Temperature and field-dependent magnetic investigation of α -Fe₂O₃/RGO nanocomposite has been carried out from 350 to 10 K. The transition of magnetic states in α -Fe₂O₃/RGO hybrid with changing temperature is discussed based on average anisotropy energy and coupling interactions. The ZFC-FC curves are also analyzed to explore the system further.

Keywords α -Fe₂O₃/reduced graphene oxide · Solvothermal technique · Magnetic characterization

The two-dimensional wonder material graphene and its derivatives have attained extensive research interests due to its unique properties and applications in almost every sphere of life. Magnetism on graphene-based materials has attracted huge research momentum for future spintronics devices, biomedical applications, and other energy storage device applications. Graphene owes long spin diffusion length, long spin lifetime arising from the weak spin-orbit, hyperfine interactions and electron mobility which can combine advantages of both charge and spin [1]. α -Fe₂O₃ is one of the transition metal oxides which has attracted significant interest for its remarkable magnetic, catalytic, optical, and electronic properties, good biocompatibility, low toxicity, and easy preparation. However, structural instability, agglomeration, poor conductivity, short hole-diffusion length, and high electron-hole recombination rate limit its applications [2]. The incorporation of reduced graphene oxide (RGO) into magnetic nanoparticles (MNPs) is of interest not only because of the stabilization of the particles but also because of the resulting magnetic properties, which can be influenced by morphologies and arrangement of both MNPs and RGO sheets. Concerning the

magnetic behavior, a percolation type of situation arises where different magnetic phases coexist in the nanocomposite. α -Fe₂O₃/RGO nanocomposite can offer unique opportunities for nanoelectronics and lightweight magnets which can open up a new way for making flexible information storage systems. The enhanced efficiency of these composites plays a key role in biomedical applications such as drug delivery, cancer treatment, sensors, water treatment, and energy storage devices [3, 4].

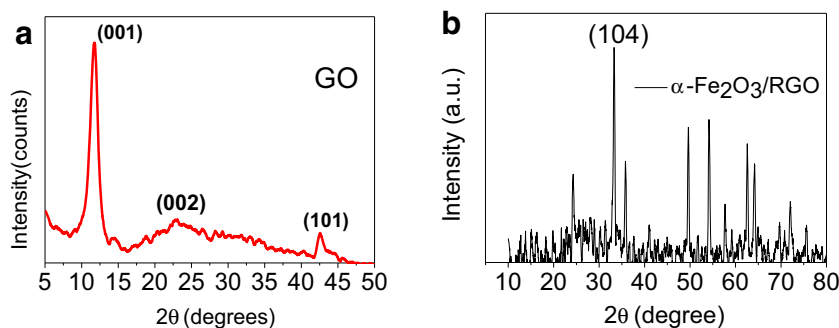
1 Experimental Details

Firstly, the graphene oxide (GO) was prepared using the modified Hummer's method from the pristine graphite powder [5]. Secondly, one step solvothermal technique was followed to synthesize α -Fe₂O₃/RGO nanocomposite. For the preparation of nanocomposite, 40 mg of GO was dispersed in 30 ml of ethanol using ultrasonication. Then, 320 mg of ferric chloride (FeCl₃ · 6H₂O) was added to GO solution. After 30 min of stirring, 960 mg of sodium acetate (NaAc) was added to the mixture solution and was stirred for 1 h. Later, this mixture was transferred to a Teflon-lined autoclave (100 ml) and subjected to a temperature of 160 °C for 24 h. After natural cooling to room temperature, the sample was collected and washed 3 times with deionized water and ethanol, respectively. Then the sample was dried under vacuum at 80 °C [3].

✉ G. Govindaraj
ggdipole@gmail.com

¹ Department of Physics, School of Physical, Chemical and Applied Sciences, Pondicherry University, R.V. Nagar, Kalapet, Pondicherry 605 014, India

Fig. 1 X-ray diffraction pattern of **a** graphene oxide and **b** α -Fe₂O₃/RGO composite



2 Results and Discussions

2.1 X-ray Diffraction Analysis

The structural phase analysis of GO, as well as α -Fe₂O₃/RGO, is accomplished using XRD and the diffraction pattern is shown in Fig. 1. The inter-planar spacing of as-prepared GO is measured using Bragg's diffraction law i.e. $2d\sin\theta = n\lambda$. For GO, a strong diffraction peak is observed at $2\theta = 11.54^\circ$ from the reflection plane (001) with a d -spacing of 7.67 Å which can be observed in Fig. 1a. Figure 1b shows the XRD pattern of α -Fe₂O₃/RGO nanocomposite. The diffraction peaks match well with pure α -Fe₂O₃ NPs and can be attributed to the rhombohedral symmetry (space group-R3c, JCPDS NO-33-0644) [5, 6]. The sharp peak at 33.45° is fitted using Gauss fit and average crystallite size is calculated using Scherer's formula as follows:

$$t = 0.9 \times \lambda / \beta \times \cos\theta \quad (1)$$

β being full-width half maxima of the fitted Gaussian peak and the crystallite size comes out to be around 27 nm. The sharp peak of GO at 11.54° at Fig. 1a is missing from the XRD pattern of α -Fe₂O₃/RGO nanocomposite indicating a successful reduction of GO to RGO [5, 7].

2.2 Scanning Electron Microscopy

The SEM image of as-prepared GO in Fig. 2a confirms the wrinkled structure of the GO surface. GO carries a good lamellar structure separated by free spaces. The layers are non-planar having a wave-like configuration. Defects present on GO surface due to the attachment of functional groups (-OH, -H, -COOH, -O-, -C, etc) and zigzag edges introduce the wrinkles and folds to sheets [5]. The image in Fig. 2b clearly shows α -Fe₂O₃ MNPs of various sizes are partially coated and irregularly decorated on the wrinkled surface of the RGO sheets. The image indicates that the RGO sheets limit the agglomeration of MNPs [3].

2.3 Raman Analysis

Raman spectra give a clear insight about the reduction of GO to RGO as well as the degree of formation of the nanocomposite. Raman spectra of GO and α -Fe₂O₃/RGO are shown in the Fig. 3 in the range of 100 to 3000 cm⁻¹ with excitation wavelength 785 nm. The Raman spectra of GO confirms two prominent bands, D band (1358 cm⁻¹) and G band (1597 cm⁻¹), which accounts for structural defects (A_{1g} mode) and sp² carbon domains (E_g mode), respectively, with intensity ratio (I_D/I_G) 0.8245. In the composite, in addition to the D and G band, ferric peaks can be observed. These are assigned

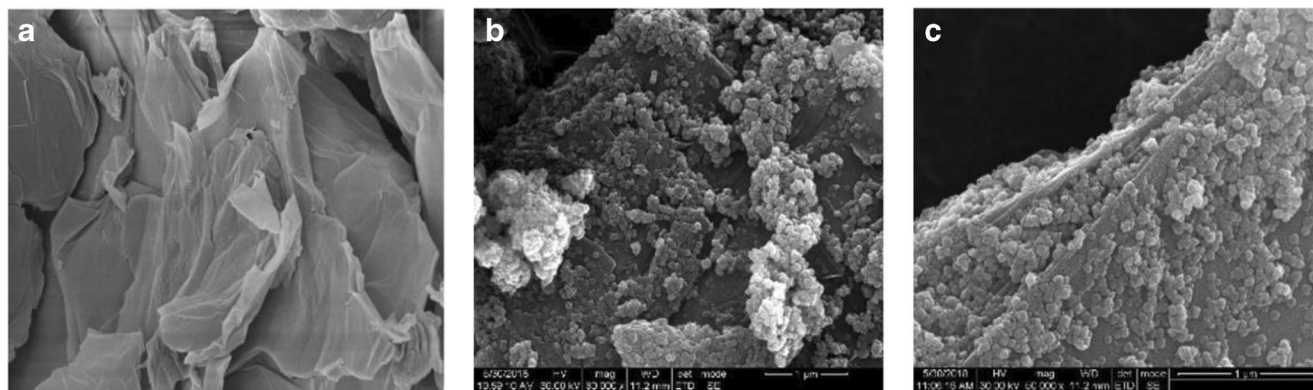


Fig. 2 SEM images: **a** GO and **b** and **c** α -Fe₂O₃/RGO nanocomposite

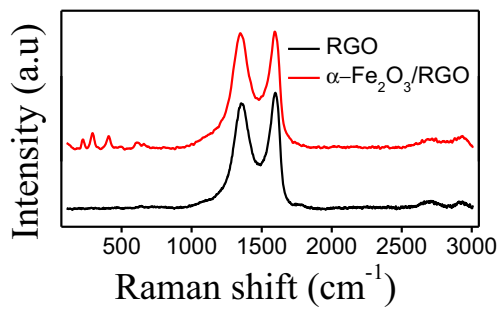


Fig. 3 Raman spectra of RGO and $\alpha\text{-Fe}_2\text{O}_3/\text{RGO}$ composite

to two classes of Raman active vibration modes, A_{1g} vibration modes (224 and 497 cm^{-1}) and E_g modes (292 , 411 and 614 cm^{-1}). The calculated I_D/I_G value is 0.9889 for the nanocomposite and the enhanced value confirmed the in situ reduction of GO to RGO as well as the existence of more surface disorders due to the anchored MNPs into the GO sheets [5, 7].

2.4 Magnetic Measurements

Field and temperature-dependent magnetic measurements of $\alpha\text{-Fe}_2\text{O}_3/\text{RGO}$ nanocomposite have been investigated using VSM probe of quantum design physical property measurement system (PPMS). Magnetic hysteresis curves are recorded at 10 K , 150 K , and 350 K and are shown in Fig. 4a–c.

In the composite, isolated $\alpha\text{-Fe}_2\text{O}_3$ MNPs along with agglomerated MNPs are arranged randomly on the amorphous RGO matrix which leads to varying volume and easy axes distribution. The $p_z\text{-}d$ orbital interaction between the RGO matrix and MNPs, RKKY type interaction between the MNPs via the conduction electrons leads to a peculiar magnetic behavior in the nanocomposite [6–8]. Ferrimagnetism is

observed up to 1 T and paramagnetism is observed above 1 T at all the three temperatures. At 10 K , in $\alpha\text{-Fe}_2\text{O}_3/\text{RGO}$ composite, spin units are independent, randomly oriented, and frozen, leading to a very less exchange interaction. At 150 K , the motion of spin units is not restricted so they can assemble forming clusters and easily interact with each other and with the RGO matrix [5]. The interparticle interaction between MNPs and interfacial interaction between the MNPs and RGO matrix grow resulting in the pinched $M(H)$. Spin coupling at the interface between RGO sheets and surface spins of MNPs causes canted spin network giving rise to exchange anisotropy. Magnetocrystalline anisotropy along with these exchange anisotropy play a significant role in the temperature dependence of magnetism in the nanocomposite. At 350 K , thermally induced disorders reshape the interactions between the spin units which results in increased pinching in the $M(H)$ curve. As the field increases above 1 T , the growing agglomeration of MNPs increase the dipolar interaction and thus anisotropy energies, resulting in paramagnetism above 1 T . We have found non-saturated $M(H)$ curves in all the three temperatures as there is a race between magnetocrystalline anisotropy with shape and stress anisotropies. Variation of coercivity with temperature is shown in Table. 1. The continuous decrease in H_c from 10 to 350 K indicates the growing interaction among MNPs and RGO matrix [9]. The increase of temperature enhances the coercivity of RGO matrix and at the same time reduces the coercivity of the $\alpha\text{-Fe}_2\text{O}_3$ MNPs. The number of MNPs being more, the Fe_2O_3 MNPs stands as a winner and decreases overall coercivity [10]. The effective saturation magnetization (M_s) at 10 K is more than 150 K and 350 K respectively and accordingly, squareness ratio (M_r/M_s) increases with the increase of temperature, which

Fig. 4 $M(H)$ curves of $\alpha\text{-Fe}_2\text{O}_3/\text{RGO}$ nanocomposite **a** at 10 K , **b** at 150 K , **c** at 350 K , and **d** ZFC-FC curves at 500 Oe

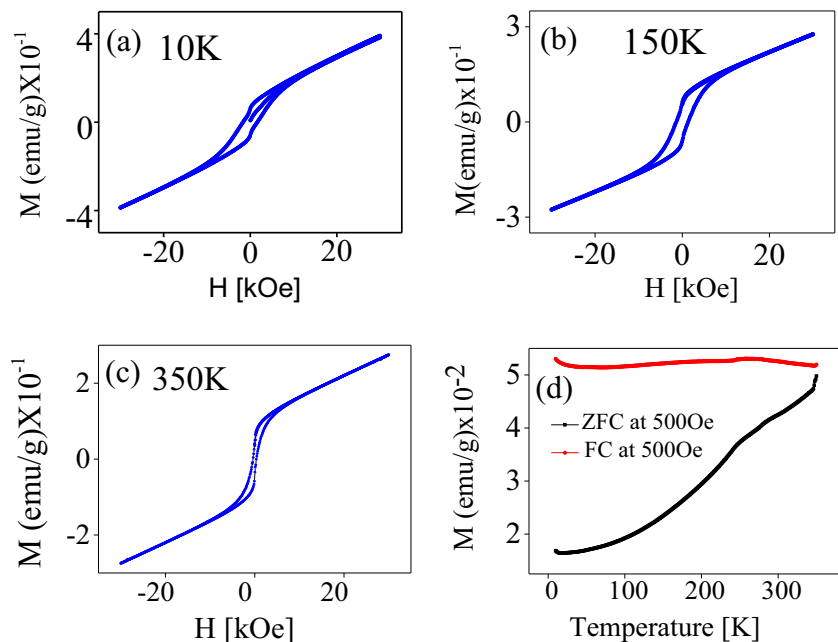


Table 1 Coercivity and remnant magnetization at 10, 150, and 350 K

Temperature (K)	Coercivity (H_c) (Oe)	Remnant magnetization (Mr) (emu/g)
	$\alpha\text{-Fe}_2\text{O}_3/\text{RGO}$	$\alpha\text{-Fe}_2\text{O}_3/\text{RGO}$
10	1648.30	5.967×10^{-2}
150	1354.66	6.076×10^{-2}
350	507.37	4.473×10^{-2}

confirms the increased exchange interaction. Figure 4 d shows the separation between ZFC and FC curves of the nanocomposite. A very less intense broad peak has been observed in ZFC around 250 K indicating the presence of bulk hematite in the system [10, 11]. The lack of bifurcation between ZFC and FC up to 350 K indicates that blocking temperature (T_B) is lying above 350 K and presence of some kind of freezing in the material due to the surface spin disorder. M_{FC} has almost nearly a constant value over the region and this value is much higher than M_{ZFC} value signifying nearly an equilibrium state. Existence of strong interaction among MNPs and between MNPs and RGO matrix brings this type of feature. M_{ZFC} is not a true equilibrium state. In the low-temperature region, the spin units have a random orientation in their easy axis directions, after applying the magnetic field (500 Oe), Zeeman energy starts aligning the spin units along with the field directions and moments increase with the temperature in the ZFC curve [11].

3 Conclusion

We have synthesized $\alpha\text{-Fe}_2\text{O}_3/\text{RGO}$ composite using the solvothermal method. GO used as a precursor was synthesized using modified Hummer's method. XRD pattern confirms the rhombohedral phase of $\alpha\text{-Fe}_2\text{O}_3$ and successful reduction of

GO to RGO. Further, Raman spectrum also points towards the formation of $\alpha\text{-Fe}_2\text{O}_3/\text{RGO}$. The transition from ferri- to paramagnetism with an increase of field in the composite is addressed using the behavior of interfacial spin units and accordingly the race between the different anisotropy energies. Further, decrease in coercivity with the increase of temperature is addressed using the interaction of moments between RGO matrix and MNPs.

Acknowledgments The authors would like to acknowledge Central Instrumentation facility (CIF), Pondicherry University for providing the characterization facility.

References

1. Li, L., Qin, R., Li, H., Yu, L., Liu, Q., Luo, G., Gao, Z., Lu, J.: ACS Nano. **5**, 2601–2610 (2011)
2. Zia, M., Phull, A.R., Ali, J.S.: Nanotechnol. Sci. Appl. **9**, 49–67 (2016)
3. Gao, Y., Wu, D., Wang, T., Jia, D., Xia, W., Lv, Y., Cao, Y., Tan, Y., Liu, P.: Electrochim. Acta. **191**, 275–283 (2016)
4. Shen, J., Hu, Y., Shi, M., Li, N., Ma, H., Ye, M.: J. Phys. Chem. **114**, 1498–1503 (2010)
5. Biswal, S., Bhaskaram, D.S., Govindaraj, G.: Mater. Res. Express. **5**, 086104 (2018)
6. Bhowmik, R.N., Saravanan, A.: J. Appl. Phys. **107**, 053916 (2010)
7. Nag, S.S., Roychowdhury, A., Das, D., Mukherjee, S.: Mater. Res. Bull. **74**, 109–116 (2016)
8. Jedrzejewska, A., et al.: J. Magn. Magn. Mater. **471**, 321–328 (2019)
9. Tadic, M., Kusigerski, V., Markovic, D., Milosevic, I., Spasojevic, V.: J. Magn. Magn. Mater. **321**, 12–16 (2009)
10. Hansen, M.F., Koch, C.B.: Phys. Rev. B - Condens. Matter Mater. Phys. **62**, 1124–1135 (2000)
11. Satheesh, M., Paloyly, A.R., Krishna Sagar, C.K., et al.: Phys. Status. Solidi. A. **215**, 1700705 (2018)

Publisher's Note Springer Nature remains neutral with regard to jurisdictional claims in published maps and institutional affiliations.